Multi-object spectroscopy using fibre optics at the Anglo-Austrialian telescope — an application to the IC 2082 galaxy cluster

- R. S. Ellis Physics Department, Durham University, South Road, Durham DH1 3LE
- P. M. Gray Anglo-Australian Observatory, PO Box 296, Epping, NSW 2121, Australia
- D. Carter Mount Stromlo and Siding Spring Observatory, Private Bag, Woden PO, ACT 2606, Australia
- J. Godwin Oxford University, South Parks Road, Oxford OX1 3RQ

Received 1983 May 16; in original form 1983 January 27

Summary. We describe a multi-object fibre optic coupler we have developed for the Cassegrain focus of the Anglo-Australian telescope. The results of a test run on the southern cluster containing the dumb-bell galaxy IC 2082 are presented. Where comparisons with previous work can be made the radial velocities determined using the coupler show no signs of any systematic errors. The new results are briefly discussed in terms of earlier claims for galactic cannibalism in the cluster.

1 Introduction

Multi-object spectroscopy via fibre optic coupling devices has been discussed by Hill et al. (1980) and by Hintzen et al. (1982). At the expense of very little effort substantial gains in observing efficiency have been realized. Here we report on the first results of a multi-object device used at the Cassegrain focus of the 3.9-m Anglo-Australian telescope (AAT) via observations of the galaxy cluster containing the giant elliptical IC 2082.

2 Techniques

2.1 GENERAL CONSIDERATIONS

A fundamental problem with developing a multi-object system on a 4-m telescope is to retain flexibility for the observer. The aim at the AAT is to provide a common-user multi-object system utilizing the particular capabilities of the AAT and its instrumentation. This instrumentation currently includes the RGO spectrograph with a wide range of dispersions (5–150 Å mm⁻¹) and the UCL Image Photon Counting System (IPCS) as the standard detector. A fixed format low dispersion CCD spectrograph with long-slit capabilities is also available.

In the first phase of this programme, described here, we use an auxiliary f/8 focus and feed fibre optic bundles from an aperture plate at this side port to an artificial fibre 'slit'; a row of fibres inside the RGO spectrograph which is mounted at the main f/8 focus. Although the field of this auxiliary focus is only $\approx 12 \, \text{arcmin}$ (compared with 40 arcmin for the main focus), it does provide the flexibility that a large spectrograph can offer and enables multi-object work without removing the spectrograph from the telescope, an important consideration for the scheduling of a large telescope where the average time allocation is ≈ 3 nights.

The long slit capability of the RGO spectrograph (3.8 cm = 4.24 arcmin) and the flexible format of the IPCS (with $\approx 5 \times 10^5$ pixels) suggest that at 33–150 Å mm⁻¹ the multi-object coupler could usefully handle up to 100 objects simultaneously if 200 μ m core (≈ 1.3 arcsec) fibres were used. However, the IPCS is magnetically focused and the present software rectifies the resulting S-distortion only over a limited area of the detector. If the fibres are close-packed along the slit the subsequent data reduction proves to be difficult, though steps are being taken to overcome this problem.

Since the observations reported here were made we and others have successfully used 50 fibres of $200 \,\mu\text{m}$ diameter and work is planned on a similar number of $400 \,\mu\text{m}$ (2.7 arcsec) fibres which are especially useful for extended objects.

Our arrangement for acquisition and guiding exploits the excellent pointing of the AAT. Fibre bundles are fed from bright fiducial stars within the field to a TV camera so that field translation and rotation can be optimized from the control room. The f/8 autoguider can also be used for long exposures. With bright objects ($B \lesssim 17$) since the IPCS has a real time display it is also possible to 'peak up' on the total spectroscopic signal. Calibration signals are provide via sources mounted inside the dome ensuring that each fibre is separately calibrated.

2.2 DETAILS OF THE FIBRE OPTIC COUPLER

The fibre bundle used for the observations discussed in Section 3 consists of lengths of Galite 4000-LC-P fibre made by Galileo Electro-optics Corp. This is a step-index, polymer-clad silica (PCS) type with a core diameter of $200\,\mu\text{m}$. A lightweight jacket of 2.5-mm diameter PVC spaghetti tubing surrounds and protects the fibre. The specified numerical aperture is 0.4 which is typical for PCS-type fibre but only a fraction of the available aperture is being used in the f/8 telescope beam.

Over 2.5-m lengths used here, the specified transmissions are 98.9 per cent at $800 \,\mu\text{m}$, 97.2 per cent at $600 \,\text{nm}$ and 92.3 per cent at $400 \,\text{nm}$. However, the major source of loss in our system results from so-called focal ratio degradation (FRD). This occurs when fibres are fed with a slow focal ratio. During transmission irregular reflections at imperfections (microbends) cause rays to be deflected and the output beam to be broadened. Tests of FRD in various PCS brands show that Galite fibres perform the best. Including Fresnel and input coupling losses for an input f/8 beam the transmission into f/8 is 45 per cent. A further loss results from pupil imagery. FRD fills in the central shadow in the Cassegrain beam and the nett transmission is reduced to 36 per cent.

The input end of each fibre was mounted in a specially constructed ferrule protecting the core and aligning the axis normal to the aperture plate. Each fibre was inserted into a fine stainless steel microtubing of outside diameter 0.5 mm. The tubing was soldered to a larger 2.5 mm diameter brass bush. The fibre core and ferrule were usually concentric to within $20 \, \mu \text{m}$.

The aperture plates were constructed from 1.6 mm brass plate. An existing 5×7 arcsec photographic plate holder was modified to mount these. At the predetermined location of

objects 0.5 mm holes were drilled to accept the ferrules using an accurate milling machine equipped with digital readouts. Drill flexure limited the positional accuracy to $20-30\,\mu\mathrm{m}$ (0.15 arcsec).

At the bundle output the fibres were mounted in a line with the output faces forming individual 200- μ m apertures to the spectrograph. The centre spacing was 1.3 mm which distributed the spectra optimally across the detector. The fibres were then epoxied into a line of 350 μ m holes drilled into another brass plate. Alignment here is critical since a shift in the beam with respect to the collimator optics introduces a loss of light. To prevent this an alignment jig was used when the fibres were being mounted.

This positioning of the bundle output meant that some of the normal spectrograph facilities (filters, arc lamp) were bypassed. By attaching small filters to individual fibres, it was possible to filter light from particular objects. A hollow cathode Cu—Ar lamp was positioned at the periphery of the central primary mirror baffle. Despite the unconventional illumination arrangement the excellent image scrambling properties of the fibres lead to a fairly uniform illumination of the spectrograph optics.

Acquisition of objects has been briefly discussed in Section 2.1. A special pair of guiding bundles was constructed to feed the telescope integrating TV system. Within a larger ferrule, seven fibres were close packed into a circular hole to achieve a central fibre surrounded by a ring of six with outside diameter of $900 \, \mu m$ (5.3 arcsec). In this way translational alignment could be achieved to better than 0.5 arcsec on 17th magnitude guide stars and by positioning the two guide ferrules at opposite sides of the aperture plate rotational alignment could be achieved to better than 0.1° .

2.3 FUTURE DEVELOPMENTS

Since these observations were made, laboratory tests have continued using the Quartz and Silica (France) series of all-silica (AS) fibres. These fibres exhibit significantly less FRD than PCS fibres. For an f/8 input, 70 per cent emerges still within f/8 (cf. 45 per cent for Galite fibres). The reduced FRD they exhibit enables them to partially transmit the central shadow reducing this loss to 10 per cent resulting in a nett system transmission of 68 per cent. The QSF-AS series is currently available in 85, 135, 200 and 400 μ m core diameters. We have chosen the wet silica version which has superior blue response at the expense of larger OH absorption bands at 750 and 950 μ m. It is likely therefore that a sensitivity gain of between 50 and 100 per cent will be possible by substituting the QSF-AS fibres in future work.

The present arrangement of directly feeding the collimator inside the RGO spectrograph is inconvenient and makes the changing of fibre bundles difficult. To overcome this problem an accessible, external focus is being built which will include shutter and filter wheel facilities. This focus will use a shorter focal length f/6 collimator mirror to accept more of the fibre output beam at the expense of slightly reduced spectral resolution.

Other developments include the modification of the coupler to the full 40 arcmin f/8 field and linkage to the fast CCD spectrograph. Close packed arrays of fibres have also been used for two-dimensional spectroscopy on extended objects, though they prove to be rather inefficient in comparison with normal long-slit spectroscopy. It may, however, be possible to achieve a high packing density of fibre cores at input in this arrangement by using polymer-clad fibres with the polymer coating replaced by a thinner layer of epoxy. Such a bundle could then be used as an 'image slicer' for high dispersion work in poor seeing. In this arrangement the fibres offer the added advantage of removing wavelength errors introduced by guiding and seeing variations.

3 Application to the IC 2082 galaxy cluster

3.1 OBSERVATIONS

As a test of the coupler described above we observed the southern cluster containing the dumb-bell galaxy IC 2082 (0428 - 5355, z = 0.040) for which some radial velocities are available and an extensive long-slit study of the central galaxy revealed evidence for galactic cannabilism (Carter *et al.* 1981).

Using a prime focus IIIa-J plate and a PDS microdensitometer, positions for a magnitude limited sample of ~ 400 galaxies were determined to a precision of ~ 0.3 arcsec rms. A finding chart for the cluster is shown in Plate 1. A sample of 21 objects (all galaxies except one compact object which turned out to be a star) with $B \le 18.75$ and within a 12 arcmin field centred on galaxy 2 was studied spectroscopically with the coupler in 1981 December. The observing record is summarized in Table 1.

Table 1. Log of observations.

Instrumentation: AAT 3.9-m, f/8 auxiliary focus RGO spectrograph 25 cm camera

Grating 600 V, dispersion 66 Å mm⁻¹, resolution 2.5 Å FWHM

λλ 4060-6136 Å

Coupler with 21 Galite 4000-LC fibres Fibre aperture: 200 µm (1.3 arcsec) diameter

Date: 1981 December 27

Exposures: 1C 2082 cluster 5000 s

Offset sky 1000 s HD 42505 1000 s

Sky spectra were obtained by offsetting the telescope rather than by dedicating one or more fibres to areas of blank sky. Although this does not provide for simultaneous sky subtraction, it does give each fibre its own sky spectrum which is more important in view of the fibre-to-fibre variations. Such variations and the compromise sky-subtraction method may limit the use of fibres for very faint objects. Sky and calibration exposures were interlaced with the cluster exposures in the usual way. Flatfield exposures were made at the start and end of the night.

3.2 DATA REDUCTION AND RESULTS

In order to wavelength calibrate each spectrum and rectify the variable S-distortion across the IPCS a two-dimensional polynomial was fitted to each calibration lamp exposure and then applied to the relevant object frame. The geometrical resampling programme was kindly supplied by C. D. Pike. Tests show that, independent of the form of the S-distortion, accuracies of < 0.2 channel rms are routinely obtained; this error is not significantly worse than that obtained with conventional spectra. Once calibrated and straightened the spectra can be extracted and treated as a normal two-dimensional array of spectra.

Radial velocities were determined using cross-correlation techniques described by Efstathiou, Ellis & Carter (1980); the star HD 42505 was used as a comparison object — its spectrum was taken through a single fibre during twilight. Heliocentric velocities and associated information are tabulated in Table 2 where we have also collated the earlier measurements. Fig. 1 shows the spectrum of a typical cluster galaxy and the cross-correlation function used to determine the radial velocity.

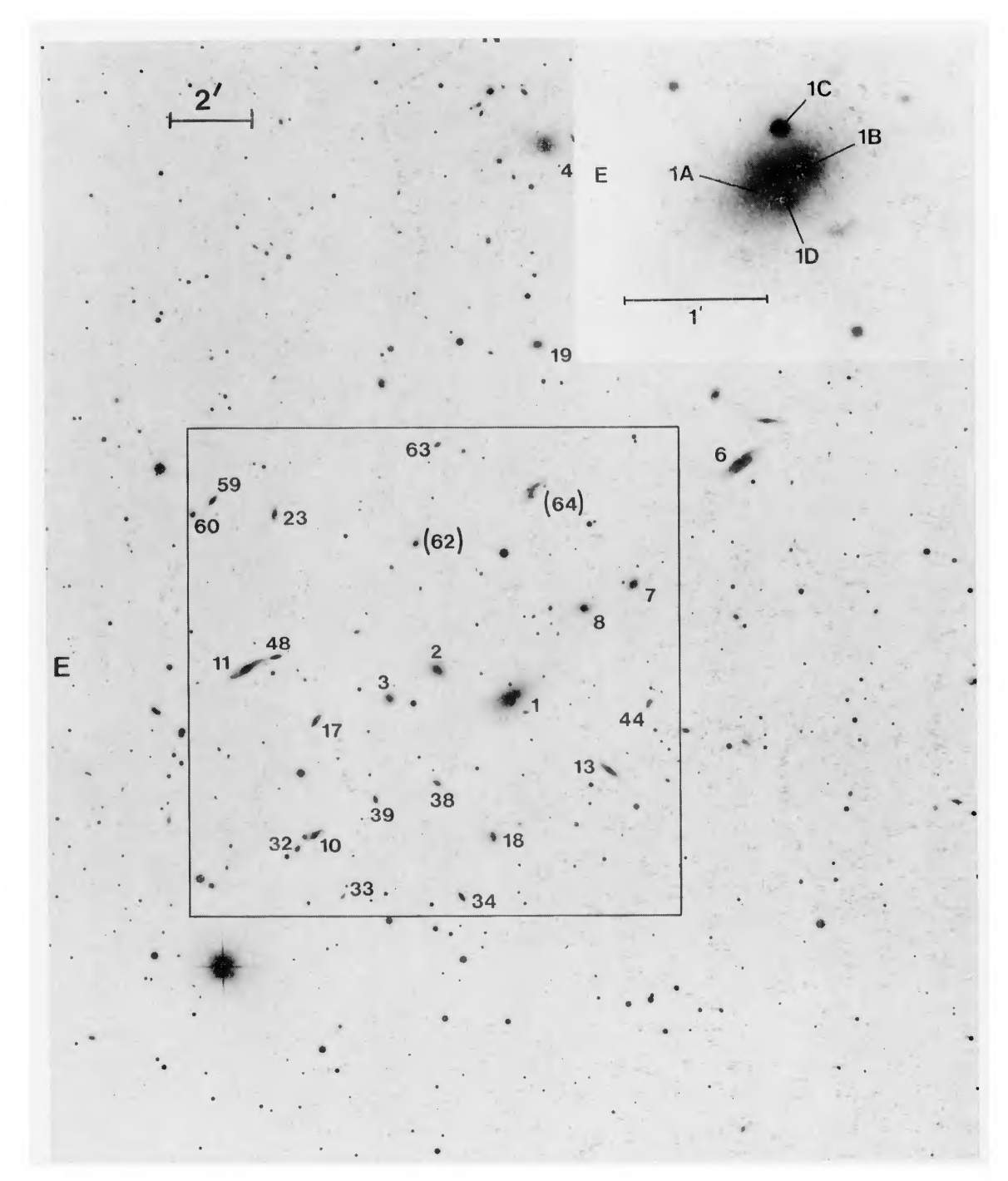


Plate 1. Finding chart for the central region of the the cluster containing IC 2082. The print is a high contrast derivative of a prime focus sky limited IIIa-J plate (kindly supplied by D. F. Malin). Galaxies 5, 9, 12, 14, 25 lie outside this field. The square defines the approximate field of the auxiliary focus. Identifications in brackets have no spectra. The inset shows the objects in the vicinity of IC 2082 as seen on a prime focus IV-N plate.

[facing page 288]

Table 2. Summary of radial velocities for IC 2082 cluster.

Object	RA (1950) (h m s)	Dec. (1950)	B	Source	CZ	r
	•					
1A	04 27 58.8	53 56 09	14.91	d	12 051	17.1
1B	04 27 57.5	53 56 05	15.92	a	11 869	4.1
				d	11 812	13.1
2	04 28 09.9	53 55 27	15.83	a	12 714	3.1
				b	12 908	4.7
3	04 28 17.6	53 56 05	16.87	a	12 108	6.0
				ь	12 165	2.9
				c	12 106	4.0
4	04 27 50.8	53 43 19	14.96	b	12 844	5.3
5	04 28 08.0	53 35 55		c	12 867	4.5
6	04 27 21.2	53 50 45	15.14	c	10 838	3.4
7	04 27 38.5	53 53 33	16.33	b	12 607	3.0
				c	12 532	3.6
8	04 27 46.4	53 54 05	16.10	a	11 558	1.9
				b	11 759	3.5
9	04 29 35.7	54 05 14		c	12 939	2.7
10	04 28 30.2	53 59 14	16.65	a	11 811	2.1
11	04 28 40.2	53 55 19	15.30	a	13 011	3.9
				c	13 028	2.6
12	04 26 24.7	54 18 23		c	1600	1.7
13	04 27 43.3	53 57 54	15.92	a	12 596	3.4
14	04 29 33.5	53 48 39		c	12 501	4.8
17	04 28 29.5	53 56 34	17.08	a	8786	1.6
18	04 28 01.9	53 59 22	16.70	a	11 126	3.7
19	04 27 52.7	53 47 56	16.33	c	12 501	4.0
23	04 28 35.0	53 51 42	16.92	a	11676	3.1
25	04 27 58.2	54 07 49	16.81	c	13 037	1.8
32	04 28 33.0	53 59 33	17.42	a	12 968	4.1
33	04 28 26.1	54 00 41	18.77	a	77 686	2.6
34	04 28 07.2	54 00 46	16.95	a	11 137	4.9
38	04 28 10.5	53 58 05	17.03	a	10523	5.2
39	04 28 20.4	53 58 26	17.38	a	12 008	3.1
44	04 27 36.7	53 56 21	17.74	a	8635	1.2
48	04 28 35.5	53 55 03	17.29	a	10 268	1.7
59	04 28 44.8	53 51 20	16.78	a	12 799	2.6
60	04 28 48.0	53 51 39	17.38	a	11 408	1.1
63	04 28 09.0	53 50 12	17.35	a	10 884	1.1

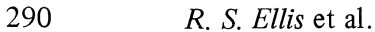
Notes

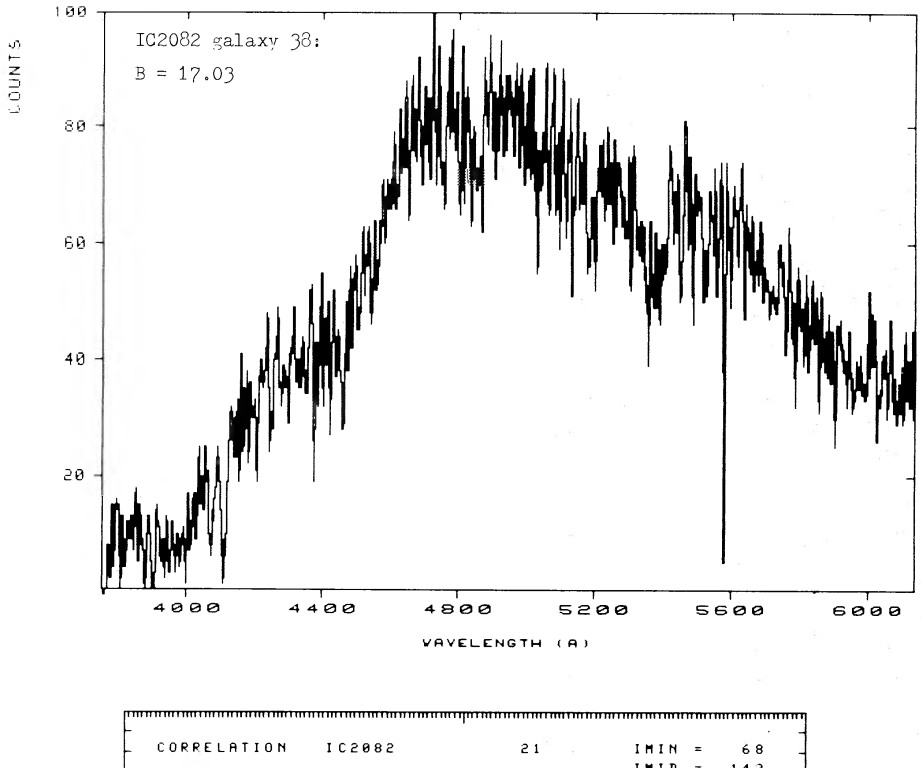
Velocities heliocentric corrected. r factor and velocity error as discussed by Tonry & Davis (1979). Code for source of velocities: a. AAT + fibres 66 Å mm⁻¹ (this paper); b. AAT + IPCS 66 Å mm⁻¹ (Carter, unpublished); c. SAAO + IPCS 50 Å mm⁻¹ (Godwin & Green, unpublished); d. AAT + IPCS 33 Å mm⁻¹ (Carter *et al.* 1981).

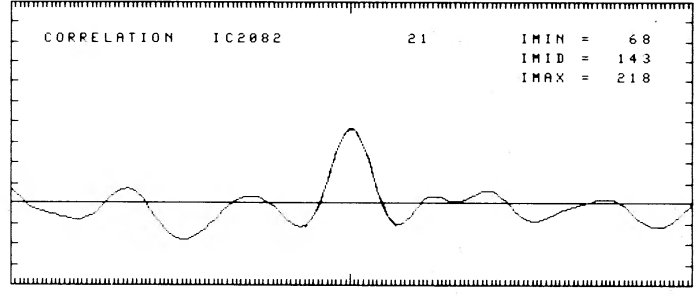
Of the 21 objects only five had been studied previously and the signal-to-noise of these observations is often poor. Using these five objects our derived (fibre) velocities show no evidence for any serious systematic errors introduced by the multi-object technique. We find

$$\langle V_{\text{fibres}} - V_{\text{other}} \rangle = -70 \pm 119 \,\text{km s}^{-1} \,(1 \,\text{sd}).$$

Using Tonry & Davis' (1979) relations for estimating the random velocity errors from the height of the cross-correlation peak we would expect a standard deviation of $\sim 95\,\mathrm{km\,s^{-1}}$. Further comparisons show the slight offset (~ 0.9 velocity channels) may arise principally in the uncertain absolute velocity scale of the earlier spectra rather than in the fibre data.







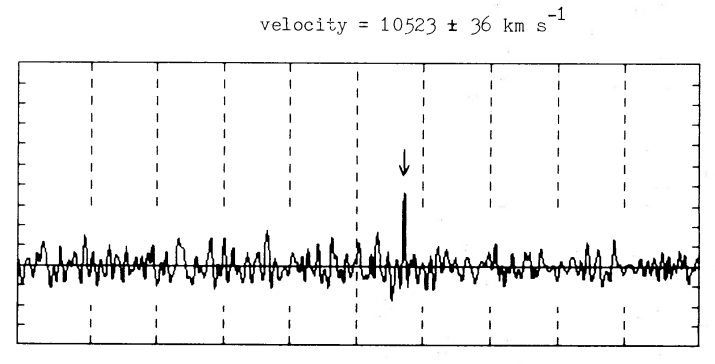


Figure 1. Wavelength calibrated spectrum (top panel) and velocity cross-correlation function (bottom panel) obtained using the fibre optic coupler for galaxy 38 in the IC 2082 cluster. The middle panel shows an enlargement of the cross-correlation function in the vicinity of the peak used to determine the radial velocity of the galaxy.

Regarding efficiency an interesting (but somewhat approximate) comparison is that of the total times involved per radial velocity (scaling for telescope apertures where necessary). Our experiment proves ≈ 8 times more efficient than previous single-object studies of this cluster (the galaxy numbers and magnitudes are comparable). Thus the relative f/8 efficiency of the fibre optic coupler using Galite fibres is ~ 40 per cent $(8 \div 21)$ in agreement with the laboratory tests discussed in Section 2.2.

The galaxy magnitudes within the 1.3 aperture are difficult to determine since they depend critically upon the seeing both on the plate used for surface photometry and on the night when the spectra were taken. As a rough guide a relationship between the aperture and isophotal magnitude was determined for ~ 200 galaxies in the cluster. The spectra we obtained then imply a count rate of $1 \, \text{s}^{-1} \, \text{Å}^{-1}$ for a star at 1 airmass with B = 14.5 (at $\lambda \, 4500 \, \text{Å}$). Comparing with recent AAO estimates of the performance of the RGO spectrograph (Hanes, private communication) this figure indicates a 35 per cent throughput for the fibre optic coupler. We stress that the recent experiments with QSF fibres (Section 2.3) provide a factor of ~ 1.5 improvement in these sensitivity estimates.

Finally we note that none of our fibre spectre has been flux calibrated. Since each fibre has its own wavelength response this would require observations of a flux standard through each fibre in turn. Furthermore laboratory tests show that the absolute response of each fibre depends slightly on the stress and curvature; the extent to which this limits spectrophotometry with such a coupler is being investigated.

3.3 DYNAMICAL IMPLICATIONS

The cluster containing IC 2082 now has radial velocity measurements for 30 galaxies including six repeated measurements (five repeats made with the fibres and one other repeat). The distribution of independent measurements is given in Fig. 2 from which it can be seen that IC 2082 itself is close to the centre of the distribution (cf. Quintana & Lawrie 1982). The mean velocity is $12\,035\,\mathrm{km\,s^{-1}}$ (cf. $12\,051$ for IC 2082) and the overall dispersion is 844 km s⁻¹. When the lowest quality spectra are rejected (Tonry & Davis' 1979 r factor r < 3.0) these values are changed to $12\,079$ and $745\,\mathrm{km\,s^{-1}}$. The new dispersion is slightly larger than the value used by Carter et al. but Fig. 2 shows that the distribution for the older data is not so well-centred around the velocity of IC 2082.

Carter et al. claimed from a long-slit study of IC 2082 that the galaxy was composed of at least two components, one having a high mass—light ratio consistent with tidally captured

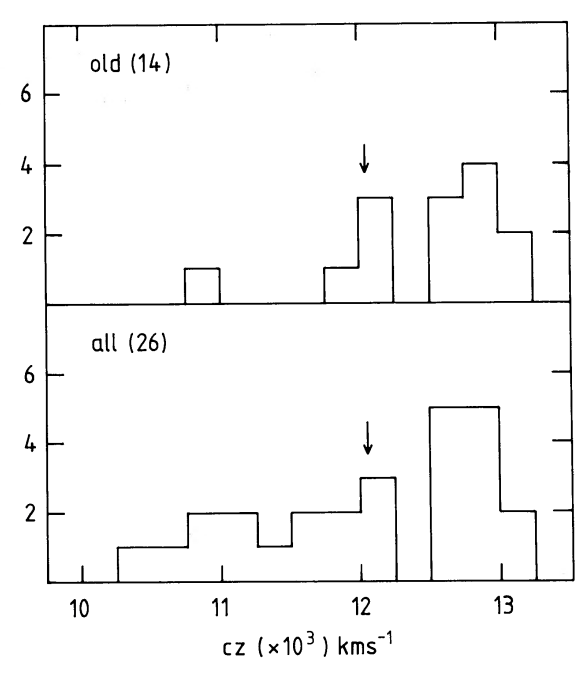


Figure 2. Distribution of radial velocities in the IC 2082 cluster. The upper panel refers to the earlier non-fibre measurements. The lower panel refers to all the independent measurements (taking fibre data in the case of repeated observations). An arrow marks the velocity of IC 2082.

debris from cluster galaxies. Inglis has re-analysed the data in terms of improved surface photometry of IC 2082, objective galaxy counts in the cluster and the new radial velocity data. A full account of these results for IC 2082 and three other cDs is given elsewhere (Inglis et al. 1984, in preparation). An appropriate two component model would be a normal elliptical with $M/L \approx 6$ and a central velocity dispersion 275 km s⁻¹ plus an outer (cluster) component with core radius 6 arcmin $(0.2\,h^{-1}\,\mathrm{Mpc})$ and dispersion 720 km s⁻¹ (rest frame). This still falls somewhat short of explaining the outermost dispersions in the long-slit data. To match the data the cluster velocity dispersion needs to be higher ($\sim 1500\,\mathrm{km\,s^{-1}}$, a point made by Carter et al.) but in view of the abundant radial velocity data that now seems unlikely. Instead, the second component has to be more concentrated with a core radius of $\sim 0.26\,h^{-1}\,\mathrm{Mpc}$. In this case the mass—light ratio of the cD rises to 32 at $15\,h^{-1}\,\mathrm{kpc}$.

Finally we note the comment by Dressler (1979) that many cD galaxies have close-by compact objects which may be remnants of galaxies whose outer envelopes have been tidally removed. In the case of IC 2082 in addition to the two nuclei A and B, whose dynamical properties were discussed by Carter et al., there are two such objects — IC and 1D in Plate 1. We can now confirm that these objects are both foreground stars.

Acknowledgments

The multi-object coupler could not have been developed without the cooperation and support of staff at the Anglo-Australian Observatory, particularly P. Gillingham, D. Morton and K. Taylor. We thank I. Inglis and C. D. Pike for assistance with software, M. Green and I. Inglis for allowing us to quote material prior to publication and acknowledge useful discussions with G. Efstathiou.

References

Carter, D., Efstathiou, G., Ellis, R. S., Inglis, I. I. & Godwin, J., 1981. Mon. Not. R. astr. Soc., 195, 15P. Dressler, A., 1979. Astrophys. J., 231, 659. Efstathiou, G., Ellis, R. S. & Carter, D., 1980. Mon. Not. R. astr. Soc., 193, 931. Hill, J. M., Angel, J. R. P., Scott, J. S., Lindley, D. & Hintzen, P., 1980. Astrophys. J., 242, 169. Hintzen, P., Hill, J. M., Lindley, D., Scott, J. S. & Angel, J. R. P., 1982. Steward Obs. Preprint No. 402 Quintana, H. & Lawrie, D. G., 1982. Astr. J., 87, 1. Tonry, J. & Davis, M., 1979. Astr. J., 84, 1511.